

Demonstration of Nonlinear Inverse Synthesis Transmission over Transoceanic Distances

Son Thai Le, *Student member, IEEE*, Ian D. Philips, Jaroslaw E. Prilepsky, Paul Harper, Andrew D. Ellis and Sergei K. Turitsyn

Abstract — Nonlinear Fourier transform (NFT) and eigenvalue communication with the use of nonlinear signal spectrum (both discrete and continuous), have been recently discussed as promising transmission methods to combat fiber nonlinearity impairments. In this paper, for the first time, we demonstrate the generation, detection and transmission performance over transoceanic distances of 10 Gbaud nonlinear inverse synthesis (NIS) based signal (4 Gb/s line rate), in which the transmitted information is encoded directly onto the continuous part of the signal nonlinear spectrum. By applying effective digital signal processing techniques, a reach of 7344 km was achieved with a bit-error-rate (BER) (2.1×10^{-2}) below the 20% FEC threshold. This represents an improvement by a factor of ~ 12 in data capacity \times distance product compared with other previously demonstrated NFT-based systems, showing a significant advance in the active research area of NFT-based communication systems.

Index Terms — Coherent, nonlinear Fourier transform, inverse scattering, orthogonal frequency division multiplexing, nonlinear signal processing, nonlinear optics.

I. INTRODUCTION

The increasing demand from the growing number of bandwidth-hungry applications and on-line services (such as cloud computing, HD video streams, on-line content sharing and many others) is pushing the required communication capacity of fiber optical systems close to the theoretical limit of a standard single-mode fiber (SSMF) [1], which is imposed by the inherent fiber nonlinearity (Kerr effect) [2]. In the last decade, extensive efforts have been made in attempting to suppress the impact of Kerr nonlinearity through various nonlinearity compensation techniques, including digital back-propagation (DBP) [3], digital [4] and optical [5-7] phase conjugations at the mid-link or installed at the transmitter [8], and phase-conjugated twin waves [9-11]. However, there are still many limitations and challenges to overcome in applying the aforementioned nonlinear compensation methods in terms of flexibility and especially the implementation complexity. As a result, further research in novel methods to combat the impairments due to fiber nonlinearity is highly desirable.

Manuscript received December 1, 2015. S. T. Le, I. D. Philips, J. E. Prilepsky, P. Harper, and S. K. Turitsyn are with Aston Institute of Photonic Technologies (AIPT), Aston Triangle, Birmingham, B4 7ET, UK (corresponding author phone: +44(0)744-702-40-09; e-mail: let1@aston.ac.uk). Copyright (c) 2015 IEEE. Personal use of this material is permitted. However, permission to use this material for any other purposes must be obtained from the IEEE by sending a request to pubs-permissions@ieee.org.

In recent years, an alternative approach of designing fiber optical communication systems [12-16], which takes into account the fiber nonlinearity as an essential element rather than a destructive effect has been actively discussed – the NFT-based approach. The main idea behind this approach is based on the fact that without perturbation the nonlinear Schrödinger equation (NLSE), which governs the propagation of optical signal in SSMF, is an integrable nonlinear system [17-19]. As a consequence of this integrability, the field evolution over the NLSE channel can be effectively presented within a special basis of nonlinear normal modes (nonlinear signal spectrum), including non-dispersive solitonic (discrete) and quasi-linear dispersive radiation (continuous) modes. The evolution of such special nonlinear modes in the fiber channel is essentially linear, which means that the nonlinearity-induced cross-talk between these modes is effectively absent during the propagation (neglecting signal corruption due to noise). As a result, the parameters of nonlinear modes can be effectively used for encoding and transmitting information in fiber channel without suffering from nonlinear crosstalk [14, 19-22]. This general idea was first introduced by Hasegawa and Nyu in [12] and was termed there as “eigenvalue communication”. There are two main directions in the NFT communications methodology categorized according to what part of the nonlinear spectrum (solitonic discrete part or continuous part) is used for the modulation and transmission. The approach of using discrete (solitonic) components of the nonlinear spectrum for data communications [16, 22-25] is often referred to as nonlinear frequency division multiplexing (NFDm) and initial experimental demonstrations have been reported recently [16, 24, 25]. In [16] the transmission of a 4 Gb/s NFDm system at 1 Gbaud in burst mode was demonstrated over 640 km. In this experiment, each burst, which carries 4 bits, contains two eigenvalues each modulated by QPSK constellations. In [24] 3-eigenvalue on-off-keyed multi-soliton NFDm signals at 0.5 Gbaud was successfully transmitted over 1800 km. However, the NFDm method requires considerable optimization of the pulse shapes for the purpose of maximizing the resulting spectral efficiency (SE) [26]. The second approach based on the modulation of the continuous part of the nonlinear spectrum, was proposed in [20] and was assessed in detail numerically in [27-30] (for optical links with ideal Raman amplification, Erbium doped fiber amplifiers (EDFAs), and non-ideal Raman amplification, respectively) – and was termed there as the nonlinear inverse synthesis (NIS) method. Recently, both the continuous and discrete parts have also been considered simultaneously [31].

In this paper, we report the first experimentally demonstration of a 10 Gbaud NFT-NIS-based signal with 120 bits/burst over a distance of 7344 km, showing a factor of 12 improvement in data capacity x distance product compared with other previously demonstrated NFT-based systems [16, 24]. We would like to stress that this is not a “hero experiment” in conventional terms, but rather an important achievement in the emerging field of the NFT transmission techniques. The obtained performance is also comparable to the performance of a conventional CO-OFDM transmission. In this experiment, the transmitted information is encoded directly onto the continuous part of the nonlinear spectrum using QPSK OFDM via an inverse NFT (INFT) [20, 27, 28, 32].

The remainder of the paper is organized as follows. An overview of NFT-based transmission is given in Section II. In Section III, the experimental setup including the transmitter, receiver, digital signal processing (DSP), and recirculating loop used to emulate transmission are described. In Sections IV and V the simulation and experimental results are presented and discussed. Section VI concludes the paper.

II. OVERVIEW OF NFT-BASED TRANSMISSION METHOD

In this section, we briefly discuss various designs of NFT-based transmission systems with a particular emphasis on NIS method. The numerical methods for calculating the NFTs can be found in [20, 22, 27, 28, 30].

A. Basics of NFT operations

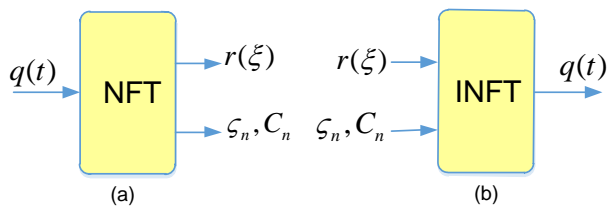


Fig. 1. Illustration of NFT and INFT for a given input the potential $q(t)$, which is assumed to decay as $t \rightarrow \pm\infty$

As explained in [20, 22, 27] and illustrated in Fig. 1, the NFT maps the initial field, $q(t)$, onto a set of scattering data $\Sigma = [(r(\xi), \xi \text{ is real}); (\xi_n, C_n)]$, where the index n runs over all discrete eigenvalues of the Zakharov–Shabat problem (if the latter are present). Herein, $r(\xi)$, ξ_n , C_n are the continuous part, discrete eigenvalues and discrete part (initial position and phases of soliton) of the signal’s nonlinear spectrum, respectively. However, within the NIS approach [27] utilized further in our paper, we deal with the soliton-free case without any discrete spectrum. As a result, the complete nonlinear spectrum consists of just the continuous part $r(\xi)$. Under the noise-free assumption, the evolution of $r(\xi)$ in lossless NLSE channel can be effectively modelled as linear all-pass filter [20, 22, 27, 28, 30]:

$$r(z, \xi) = r(0, \xi) \cdot e^{-2j\xi^2 z}. \quad (1)$$

This remarkable property makes the continuous part of the signal’s nonlinear spectrum ideal information carriers in nonlinear fiber channels.

B. NFT-based system designs

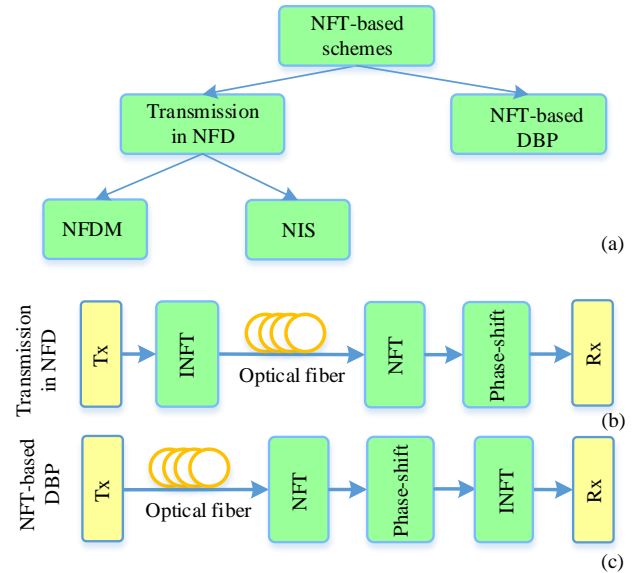


Fig. 2. Basic designs of NFT-based transmission systems (a); transmission in the nonlinear Fourier domain (NFD) (b); nonlinear Fourier domain based DBP (NFD-DBP) (c).

The basic designs and concept of NFT-based transmission systems are presented in the Fig. 2, where yellow blocks (Tx/Rx) indicate the conventional Tx/Rx. In general, NFT-based transmission systems can be divided into two major groups, which can be referred to as transmission in the nonlinear Fourier domain (NFD) and NFT-based DBP. In the first design (Fig. 2(b)), the transmitted information is encoded directly onto the nonlinear signal spectrum (discrete and/or continuous parts) via the INFT. So far, the modulations of continuous spectrum [20, 27], discrete spectrum [24–26] are often considered separately due to the numerical complexity of the full NFT-INFT cycle. The resulted transmission methods are usually termed as NIS and NFD, respectively. In the second design (Fig. 2(c)), the NFTs are used to cancel the nonlinearity distortion in fiber optical communication systems. This can be effectively achieved in the nonlinear Fourier domain with single-tap phase-shift removal as the evolution of nonlinear spectrum is trivial [19, 33].

In NFD transmissions, if only one purely imaginary eigenvalue is modulated with on-off keying signal the resulted transmission scheme converges to the conventional soliton transmission scheme. In this case, the transmitted signal can be detected at the receiver without NFT operation (using the conventional time domain sampling receiver). In general, NFD can be considered as multi-soliton transmission scheme, where one or more solitons, which are modulated in amplitude (imaginary part of eigenvalues), frequency (real part of eigenvalues) or initial position (discrete part, C_n), are transmitted simultaneously in one burst.

On the other hand, in comparison to NFD, NIS is an orthogonal approach, where the vast amount of available degrees of freedom contained in the continuous part of the nonlinear spectrum is exploited for data transmission. As a result, various conventional modulation formats, such as QAMs, can be effectively combined with the NIS method,

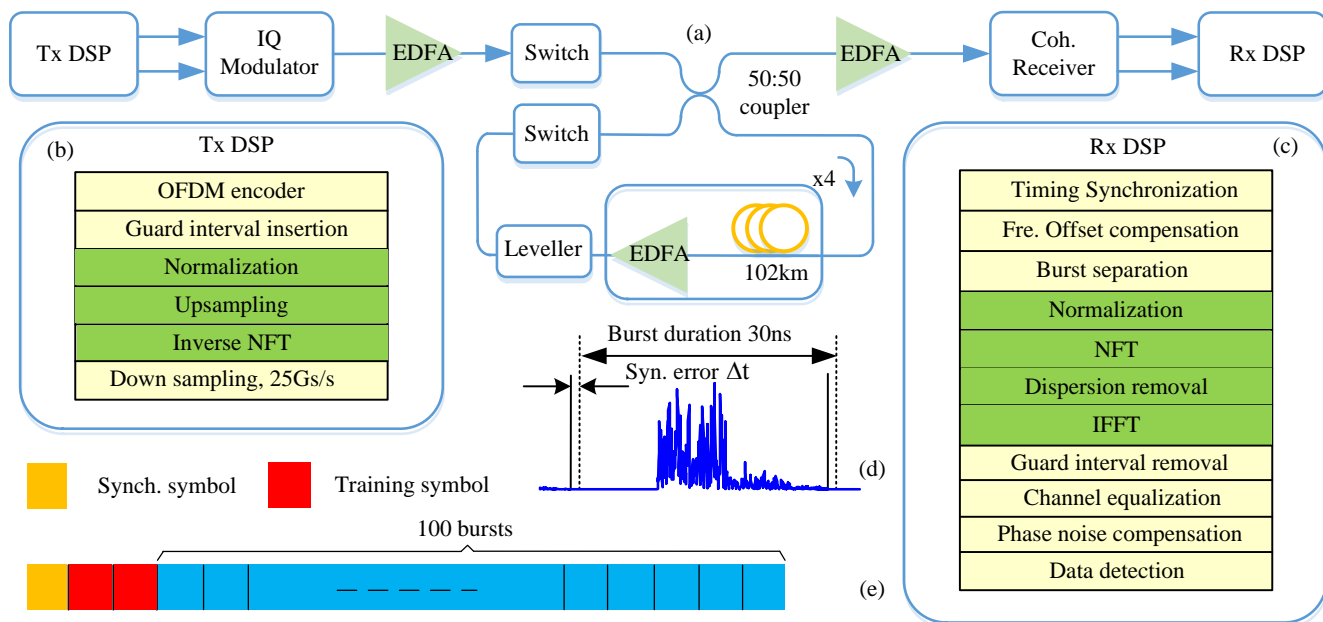


Fig. 3(a): Schematic of the experimental setup of 10 Gbaud NIS-based transmission in fibre link with EDFA-only amplification; (b) – block diagram of the Tx DSP; (c) – block diagram of the Rx DSP; (d) – illustration of a transmitted burst with a duration of 30ns carrying 120 bits (60 QPSK symbols) and illustration of synchronization error, (e) - structure of the transmitted signal, including one synchronization symbol, two training symbols for channel estimation and 100 OFDM NIS-based bursts.

providing the flexibility in the system’s design for achieving a high SE [20, 27, 28, 30]. In addition, NIS is a fully DSP-based approach, and thus, it can be easily integrated with the current coherent transmission technology. Finally, the numerical complexity of NIS, which is independent to the transmission distance, can be competitive and potentially even outperform that of the digital back propagation (DBP) based methods [27]. Therefore, in this work we focus only on NIS-based transmission schemes.

III. EXPERIMENTAL SETUP OF 10 GBAUD OFDM NIS-BASED TRANSMISSION

To demonstrate the possibility of encoding and detecting information using the signal’s nonlinear spectrum we have designed a 10 Gbaud NIS-based system in burst mode and experimentally evaluated its transmission performance over transoceanic distances.

A. Tx DSP and setup

The schematic of the experimental setup, together with the Tx, Rx DSP are shown in the Fig. 3(a-c), where the green blocks indicate the required additional DSP blocks for NIS-based transmission. For each burst and each predefined launch power, a 10 Gbaud OFDM waveform (one OFDM symbol, 6 ns of duration, no cyclic prefix) was generated offline using an IFFT (size of 128), where 60 subcarriers were filled with QPSK data and the remaining subcarriers were set to 0 for oversampling purposes. Guard bands of 12 ns were added to both the beginning and the end of the OFDM symbol to avoid inter-burst interference effects, giving a total burst period of 30 ns (the bit-rate is 4 Gb/s). The generated signal was then normalized using the lossless path average NLSE model for optical links with lumped amplification [28]. The resulting signal was upsampled (by a factor of 10 times) before being

fed into the INFT block. Herein, the INFT maps the linear spectrum of the input signal to the continuous part of the nonlinear spectrum of the output signal [20, 27]. Since the OFDM waveform was used as the input signal of the INFT block, the continuous part of the nonlinear spectrum of the output signal was directly modulated by QPSK data. Upsampling is necessary here to reduce the error associated with the INFT. Finally, the generated signal after INFT was downsampled to 25 Gs/s before being loaded into the arbitrary waveform generator (AWG) with a DAC providing around 5.6 bits of effective resolution (over a bandwidth of 12.5GHz) and fed through a linear amplifier to drive an IQ modulator.

B. Recirculating loop

The transmission experiment used a re-circulating loop consisting of a 4×102 km span single mode Sterlite OH-LITE (E) fiber (~17.5 ps/nm.km of dispersion, ~ 19 dB insertion losses per span of 102 km) and a gain flattening filter (leveller), acting as a bandpass filter. In addition to the channel under test, we used 10 loading channels with ~5 nm guard band in each side. The signals were amplified in EDFAs with a noise figure of 6 dB. At the receiver, the channel under test was filtered and amplified (using a low-gain EDFA) before being coherently detected using a real-time 80 Gs/s sampling oscilloscope. Both the transmitter laser and local oscillator were external cavity lasers each with a linewidth of ~100 kHz.

C. Rx DSP

The Rx DSP (Fig. 3c) firstly used a training symbol to perform both timing synchronization and frequency offset compensation. The signal was then separated into a number of discrete 30 ns bursts before being normalised according to the lossless path averaged model [28]. The normalized power was adjusted to be slightly different from the actual launch power

to account for the power variation during each re-circulation resulting from wavelength dependent gain-loss imperfections. After normalization, the NFT was performed to recover the continuous part of signal's nonlinear spectrum and single-tap dispersion compensation was performed to remove the effects of both the chromatic dispersion and fibre nonlinearity:

$$r^{eq}(\xi) = r(z, \xi) \cdot e^{2j\xi^2 z} \quad (2)$$

Next, the IFFT was performed to recover the transmitted time domain signal and then the guard bands were removed and the resulting signal was fed into the traditional OFDM receiver. For the NIS-based systems, synchronization error (Δt) will result in a frequency dependent phase shift in the nonlinear Fourier domain:

$$r(q(t - \Delta t), \xi) = e^{-2j\xi\Delta t} r(q(t), \xi), \quad (3)$$

where $r(q(t), \xi)$ is the continuous part of the nonlinear spectrum of the signal $q(t)$.

Since the synchronization error is constant for all bursts in one frame, the resulting frequency dependent phase shift can be readily corrected through a single-tap channel estimation and equalization using training sequences. Herein, the first two bursts were used for channel estimation (Fig. 3(e)). The impact of laser phase noise was compensated after channel estimation using 4 pilot subcarriers in each OFDM burst. We corrected for the common phase error only, the impact of which on the NIS-based systems is similar to those of the conventional linear transmission schemes. Finally, the system performance was evaluated directly from the BER by processing 10 recorded traces (each with 100 bursts), and the results are expressed as a Q factor.

IV. SIMULATION RESULTS

In general, NIS-based transmission scheme can be understood as a nonlinear pre-distortion technique. At the transmitter, the

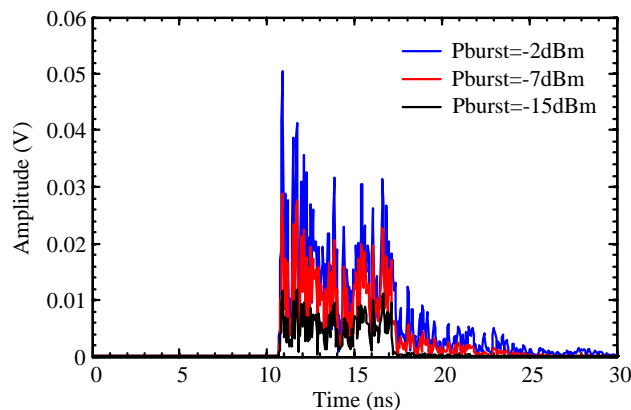


Fig. 4. Comparison of output signals of the INFT block given the same input 10 Gbaud OFDM waveform with different power levels.

linear spectrum of an encoded signal is mapped to the continuous part of the nonlinear spectrum of another signal to be transmitted over the fiber link [27, 28]. As this mapping operation is nonlinear, the generated signal via the INFT block strongly depends on the input's signal power. In Fig. 4, different output signals of the INFT block given the same input

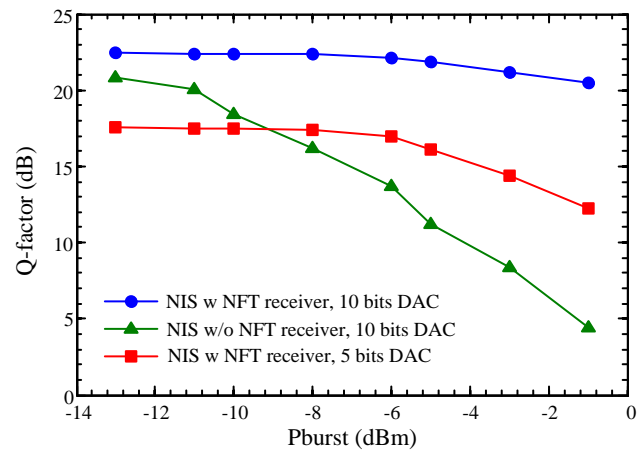


Fig. 5. Simulated back-to-back performance of NIS-based 10 Gbaud OFDM system at 25 Gs/s with and without NFT receiver. The DAC resolutions are 5 and 10 bits, no noise was added.

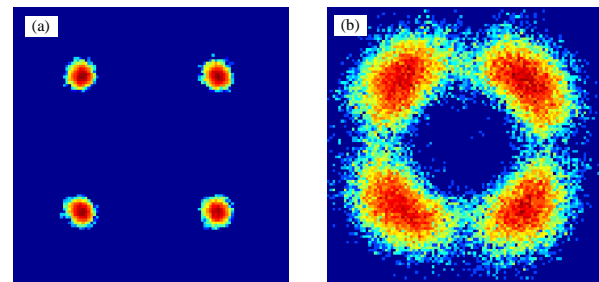


Fig. 6. Received constellations of NIS-based 10 Gbaud OFDM system at 25 Gs/s with and without NFT receiver, Pburst = -3dBm.

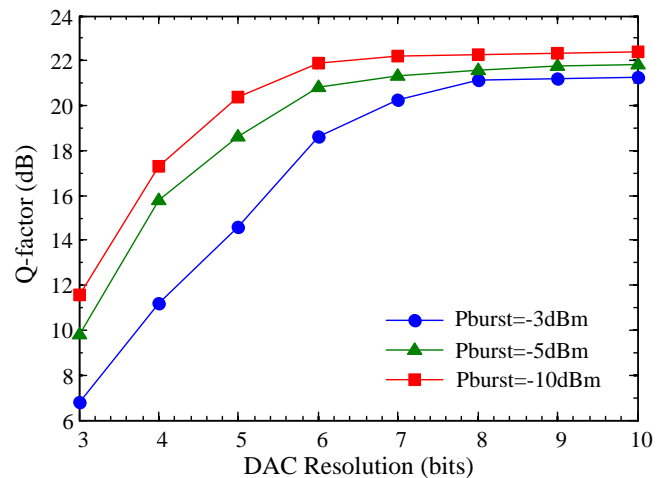


Fig. 7. Simulated back-to-back performance of NIS-based 10 Gbaud OFDM system sampling at 25 Gs/s with different values of the burst power the Tx DAC resolutions.

OFDM waveform with different power levels are compared. It can be seen that, as the input signal power is increased, the amount of signal's energy contained in the decaying tail generated after INFT also increases. This long decaying tail tightens the DAC resolution requirement in NIS-based transmission systems. In this work, we assume that the signal's energy contained in the tail generated after INFT is small enough and can be eliminated when defining the effective burst power in following discussions. Herein, the effective

burst power is defined as the ratio of the total signal energy within a burst to the initial signal duration (before INFT, 6 ns). One important property of the nonlinear spectrum is that the discrete part is absent and the continuous part converges to the ordinary Fourier transform at low power values [20, 22, 27]. As a result, at low signal power values, the traditional receiver (without NFT and IFFT blocks, Fig. 3(c)) can also be used in NIS-based transmissions. However, as the signal power is increased the continuous part of the signal's nonlinear spectrum diverges to its linear counterpart leading to performance penalty if the conventional receiver (without NFT) is employed.

Extensive simulations were performed to understand the performance penalty associated with a conventional OFDM receiver and the finite DAC resolution. In simulation, the system performance was evaluated through error vector magnitude and then was converted to Q-factor for comparison purposes. In Fig. 5 the back-to-back performances of NIS-based 10 Gbaud OFDM systems sampled at 25 Gs/s with and without NFT receivers are compared. To eliminate the impact of DAC resolution, we first considered a high DAC resolution of 10 bits. In Fig. 5, if the NFT receiver is employed (blue curve with circle marker), only slight performance degradation (~2 dB) is observed if the burst power is increased from -13 dBm up to -1 dBm. The performance degradation is due to the fact that increasing the signal power leads to a longer decaying tail, a part of which falls outside the burst duration of 30 ns and is truncated. When the conventional receiver (without NFT) is employed, the performance penalty significantly increases with the increasing of the burst power. This clearly indicates that the NFT receiver is mandatory for the NIS-based systems operating with medium-to-high signal power. The received constellations of NIS-based 10 Gbaud OFDM systems with and without NFT receiver are compared in Fig. 6, for a burst power of -3dBm.

If the DAC resolution is reduced to a practical value of 5 bits, a significant performance penalty can be observed, ranging from ~5 dB for -13 dBm burst to ~8 dB for a -1dBm burst. This result clearly indicates that the performance penalty due to a low DAC resolution increases with the growth of the burst power. We believe that this is due to the fact that a higher DAC resolution is required to preserve the longer decaying tail when the burst power is increased.

The performances of NIS-based 10 Gbaud OFDM systems as functions of the DAC resolution for different burst power values are plotted in Fig. 7. In this figure the required DAC resolutions for negligible performance penalty are 6 bits, 7 bits and 8 bits for $P_{burst} = -10$ dBm, -5 dBm and -3 dBm, respectively.

V. EXPERIMENTAL RESULTS

A. Back-to-back performance

The performances of OFDM systems with and without NIS as functions of OSNR for different burst power values are given in Fig. 8, where closed symbols and solid lines with open symbols depict the experimental and simulation results, respectively. At a low burst power value the OSNR penalty

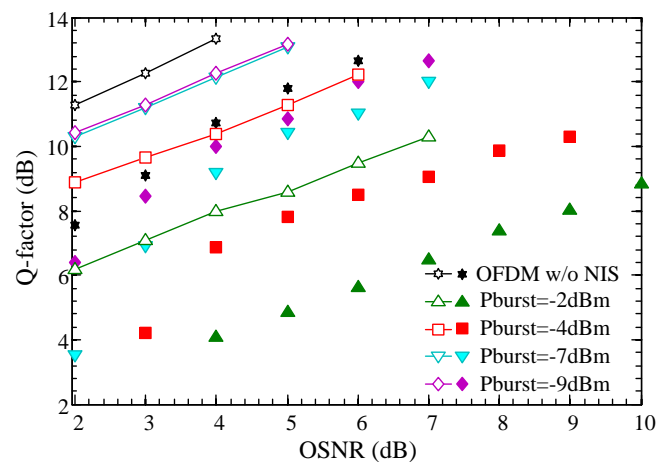


Fig. 8. Back-to-back performances of 10 Gbaud OFDM and NIS-based OFDM systems for different burst power values. Closed symbols are experimental data. The solid lines with open symbols are simulation results, the DAC resolution was set to 5 bits.

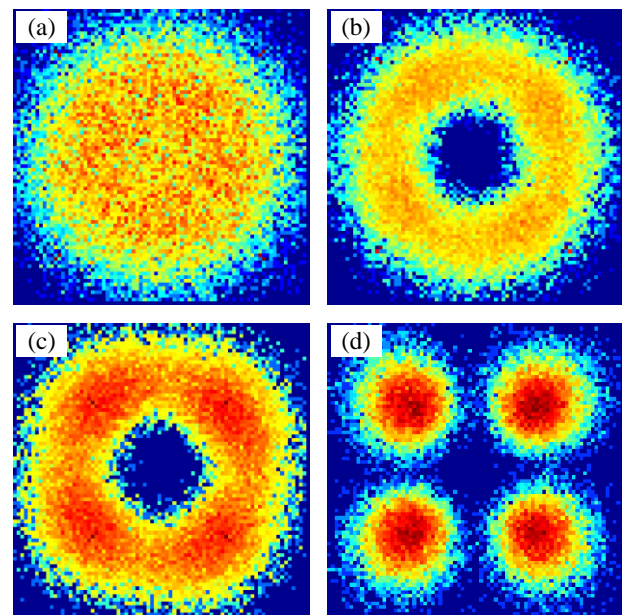


Fig. 9. Constellation diagrams at the burst power of -5dBm after 4080 km of transmission distance, (a) – before dispersion removal, (b) – before channel estimation, (c) – before phase noise compensation, (d) – final constellation after phase noise compensation

compared with the conventional OFDM system (with the same parameters) is as small as 1dB. However, the OSNR penalty of the NIS-based system increases quickly with the rise of the burst power. At a high burst power value of -2 dBm, a BER level of 10^{-3} ($Q \sim 9.8$ dB) could not be achieved. As discussed above, we attribute this phenomenon to the fact that a higher burst power requires a higher DAC resolution due to the longer decaying tail. As a result, with a fixed DAC resolution (~5.6 bits) and a fixed guard interval duration, the OSNR penalty increases with the rise of the burst power.

This phenomenon can also be confirmed by simulation results presented in Fig. 8, where the OSNR penalty increases significantly with the rise of the burst power (the effective DAC resolution was fixed at 5 bits). In comparison to

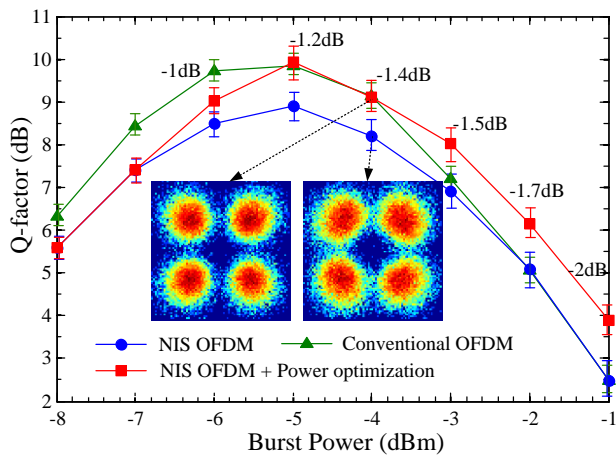


Fig. 10. Q-factor as a function of the burst power after 4080 km. The numbers are power correction values for each burst power value.

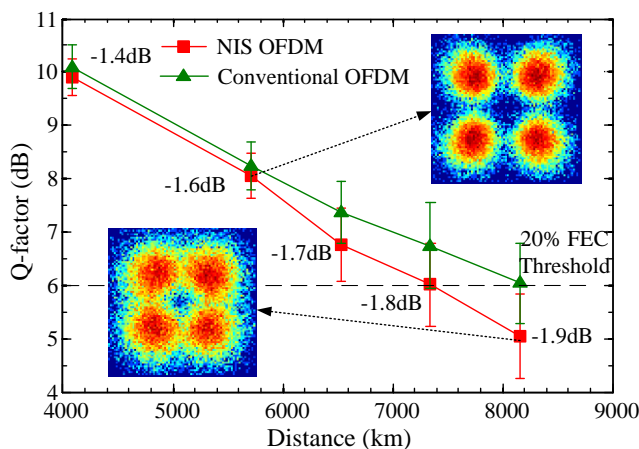


Fig. 11. Optimum Q-factor as functions of the transmission distance. The numbers are power correction values for each distance value at the optimum burst power.

simulation results obtained with ideal Rx and Tx with a limited DAC resolution as the only impairment, the implementation penalty also increases with the rise of the burst power. This result clearly suggests that NIS-based systems are also very sensitive to other transceiver imperfections such as Rx ADC resolution, DAC, ADC transfer functions and laser phase noises. As a result, novel and effective transceivers' equalization techniques are desirable to minimize the back-to-back implementation penalty. This is an important topic for future research.

B. Experimental transmission performance

Typical constellation diagrams after several receiver DSP blocks, including single-tap dispersion removal, channel estimation, and phase noise estimation, are presented in Fig. 9 for the burst power of -5 dBm after a distance of 4080 km. At each step, the constellation was achieved by feeding the obtained signal directly into the conventional OFDM receiver. After the single tap dispersion removal, a clear open "eye" can be observed (Fig. 9(b)). Next, channel estimation was performed to remove the frequency dependent phase-shift due to synchronization error. The obtained constellation, Fig. 9(c), clearly shows that the synchronization error induced phase-shift was effectively removed. The final constellation diagram,

Fig. 9(d), indicates that the transmitted QPSK data was successfully recovered.

The performance of the conventional OFDM system (without NFTs at both Tx and Rx) and the NIS-based OFDM system are compared in Fig. 10 for the 4080 km distance. If the receiver normalized power was set to be equal to the launch power, the optimum Q-factor was found to be ~ 9 dB (blue curve), which is ~0.9 dB worse than the conventional OFDM system. However, by adjusting the normalized power an additional 1 dB gain in Q-factor can be achieved (red curve), which is comparable to the conventional OFDM system. At the launch power of -5 dBm, the optimum receiver normalised power was -6.2 dBm. The power correction value in this case was -1.2 dB. We attribute this phenomenon to the gain-loss imperfection of the loop due to non-optimized setting of the leveller and EDFA gain reduction caused by the accumulation of ASE noise during the recirculation. The gain-loss imperfection leads to the power variation after each recirculating loop, degrading the accuracy of the nonlinear pre-distortion technique. In the highly nonlinear regime, by optimizing the normalized power the NIS-based OFDM system shows up to 2 dB performance advantage over the conventional OFDM system, and 1 dB increase in the nonlinear threshold. We believe that the low DAC resolution hinders the observation of further performance benefit of NIS-based system, although parametric noise amplification [34] and the finite guard interval may also contribute to performance degradation.

The optimum Q-factors as functions of transmission distance is depicted in Fig. 11, for NIS-based and the conventional OFDM systems. We see equal performance over both systems to ~5700km, where the conventional system starts to outperform the NIS-based system. Again this is thought to be due to the reasons outlined above. After propagation over 18 loops (7344 km) the BER obtained (2.1×10^{-2}) was below 20% FEC threshold. This result indicates the record distance reach of any NFT-based systems up date. Taking into account the expected uncertainty in measured Q factor from the finite sample size, we believe that these results are close to those observed for conventional OFDM.

VI. CONCLUSION

We have experimentally demonstrated the record distance reach (7344 km at $\text{BER}=2.1 \times 10^{-2}$) of any NFT-based systems by encoding and detecting information on/from the continuous part of the nonlinear signal spectrum using the NIS-based transmission ideology [20, 27, 28]. In comparison with the conventional system, the NIS-based system shows up to 2 dB performance gain in the highly nonlinear regime. However, the overall system performance benefit is hindered by the transceiver's imperfections, the low DAC resolution and other system design's constrains, leaving good potential for further system performance improvement using NFT technique. These preliminary results are very close to conventional OFDM, and we anticipate that addressing the system imperfections outlined above will enable net performance gains to be observed when comparing NIS and conventional transmission schemes. Alongside with this, our results have also revealed the

potential of using the continuous nonlinear spectrum part for the transmission purposes.

ACKNOWLEDGMENT

This work was supported by the UK EPSRC Grants UNLOC (EP/J017582/1) and PEACE (EP/L000091/1). The authors thank Sterlite Technologies for their support.

REFERENCES

- [1] A. D. Ellis, Z. Jian, and D. Cotter, "Approaching the Non-Linear Shannon Limit," *Journal of Lightwave Technology*, vol. 28, pp. 423-433, 2010.
- [2] R. Essiambre, G. Kramer, P. J. Winzer, G. J. Foschini, and B. Goebel, "Capacity Limits of Optical Fiber Networks," *Journal of Lightwave Technology*, vol. 28, pp. 662-701, 2010.
- [3] E. Ip and J. M. Kahn, "Compensation of Dispersion and Nonlinear Impairments Using Digital Backpropagation," *Journal of Lightwave Technology*, vol. 26, pp. 3416-3425, 2008/10/15 2008.
- [4] X. Chen, X. Liu, S. Chandrasekhar, B. Zhu, and R. W. Tkach, "Experimental demonstration of fiber nonlinearity mitigation using digital phase conjugation," in *Optical Fiber Communication Conference and Exposition (OFC/NFOEC), 2012 and the National Fiber Optic Engineers Conference*, 2012, pp. 1-3.
- [5] S. L. Jansen, D. Van den Borne, B. Spinnler, S. Calabro, H. Suche, P. M. Krummrich, et al., "Optical phase conjugation for ultra long-haul phase-shift-keyed transmission," *Journal of Lightwave Technology*, vol. 24, pp. 54-64, 2006.
- [6] D. M. Pepper and A. Yariv, "Compensation for phase distortions in nonlinear media by phase conjugation," *Optics Letters*, vol. 5, pp. 59-60, 1980/02/01 1980.
- [7] I. Phillips, M. Tan, M. F. Stephens, M. McCarthy, E. Giacomidis, S. Sygletos, et al., "Exceeding the Nonlinear-Shannon Limit using Raman Laser Based Amplification and Optical Phase Conjugation," in *Optical Fiber Communication Conference*, San Francisco, California, 2014, p. M3C.1.
- [8] S. Watanabe, S. Kaneko, and T. Chikama, "Long-Haul Fiber Transmission Using Optical Phase Conjugation," *Optical Fiber Technology*, vol. 2, pp. 169-178, 4// 1996.
- [9] X. Liu, S. Chandrasekhar, P. J. Winzer, R. W. Tkach, and A. R. Chraplyvy, "Fiber-Nonlinearity-Tolerant Superchannel Transmission via Nonlinear Noise Squeezing and Generalized Phase-Conjugated Twin Waves," *JLT*, vol. 32, pp. 766-775, 2014.
- [10] S. T. Le, M. E. McCarthy, N. M. Suibhne, A. D. Ellis, and S. K. Turitsyn, "Phase-Conjugated Pilots for Fibre Nonlinearity Compensation in CO-OFDM Transmission," *Journal of Lightwave Technology*, vol. 33, pp. 1308-1314, 2015.
- [11] S. T. Le, M. E. McCarthy, N. M. Suibhne, M. A. Z. Al-Khateeb, E. Giacomidis, N. Doran, et al., "Demonstration of Phase-Conjugated Subcarrier Coding for Fiber Nonlinearity Compensation in CO-OFDM Transmission," *Journal of Lightwave Technology*, vol. 33, pp. 2206-2212, 2015.
- [12] A. Hasegawa and T. Nyu, "Eigenvalue communication," *Journal of Lightwave Technology*, vol. 11, pp. 395-399, 1993.
- [13] J. E. Prilepsky and S. K. Turitsyn, "Eigenvalue communications in nonlinear fiber channels," in *Odyssey of Light in Nonlinear Optical Fibers: Theory and Applications*, ed: eds. K. Porsezian and R. Ganapathy, (CRC Press, 2015). 2015, pp. 459-490.
- [14] M. I. Yousefi and F. R. Kschischang, "Information transmission using the nonlinear Fourier transform, Part III: Spectrum modulation," *IEEE Trans. Inf. Theory.*, vol. 60, pp. 4346- 4369, 2014.
- [15] A. Maruta, "Eigenvalue Modulated Optical Transmission System," presented at the OECC, Shanghai, China, 2015.
- [16] V. Aref, H. Bülow, K. Schuh, and W. Idler, "Experimental Demonstration of Nonlinear Frequency Division Multiplexed Transmission," presented at the ECOC, Valencia, Spain, 2015.
- [17] A. H. a. Y. Kodama, *Solitons in Optical Communications* Oxford University Press, 1996.
- [18] V. E. Zakharov and A. B. Shabat, "Exact theory of two-dimensional self-focusing and one-dimensional self-modulation of waves in nonlinear media," *Soviet Physics-JETP*, vol. 34, pp. 62-69, 1972.
- [19] E. G. Turitsyna and S. K. Turitsyn, "Digital signal processing based on inverse scattering transform," *Opt. Lett.*, vol. 38, pp. 4186-4188, 2013.
- [20] J. E. Prilepsky, S. A. Derevyanko, K. J. Blow, I. Gabitov, and S. K. Turitsyn, "Nonlinear inverse synthesis and eigenvalue division multiplexing in optical fiber channels," *Phys. Rev. Lett.*, vol. 113, 2014.
- [21] J. E. Prilepsky, S. A. Derevyanko, and S. K. Turitsyn, "Nonlinear spectral management: Linearization of the lossless fiber channel," *Optics Express*, vol. 21, pp. 24344-24367, 2013/10/07 2013.
- [22] M. I. Yousefi and F. R. Kschischang, "Information transmission using the nonlinear Fourier transform, Part I: Mathematical tools," *IEEE Trans. Inf. Theory.*, vol. 60, pp. 4312 - 4328, 2014.
- [23] H. Buelow, "Experimental Assessment of Nonlinear Fourier Transformation Based Detection under Fiber Nonlinearity," presented at the ECOC, Cannes, France, paper We.2.3.2, 2014.
- [24] Z. Dong, S. Hari, G. Tao, Z. Kangping, M. I. Yousefi, L. Chao, et al., "Nonlinear Frequency Division Multiplexed Transmissions Based on NFT," *PTL, IEEE*, vol. 27, pp. 1621-1623, 2015.
- [25] H. Terauchi and A. Maruta, "Eigenvalue modulated optical transmission system based on digital coherent technology," in *OptoElectronics and Communications Conference held jointly with 2013 International Conference on Photonics in Switching (OECC/PS), 2013 18th*, 2013, pp. 1-2.
- [26] S. Hari, F. Kschischang, and M. Yousefi, "Multi-eigenvalue communication via the nonlinear Fourier transform," in *Communications (QBSC), 2014 27th Biennial Symposium on*, 2014, pp. 92-95.
- [27] S. T. Le, J. E. Prilepsky, and S. K. Turitsyn, "Nonlinear inverse synthesis for high spectral efficiency transmission in optical fibers," *Opt. Express*, pp. 26720-26741, 2014.
- [28] S. T. Le, J. E. Prilepsky, and S. K. Turitsyn, "Nonlinear inverse synthesis technique for optical links with lumped amplification," *Optics Express*, vol. 23, pp. 8317-8328, 2015/04/06 2015.
- [29] S. T. Le, J. E. Prilepsky, M. Kamalian, P. Rosa, M. Tan, J. D. Ania-Castañón, et al., "Modified Nonlinear Inverse Synthesis for Optical Links with Distributed Raman Amplification," presented at the ECOC, Valencia, Spain, 2015.
- [30] S. T. Le, J. E. Prilepsky, P. Rosa, J. D. Ania-Castanon, and S. K. Turitsyn, "Nonlinear Inverse Synthesis for Optical Links with Distributed Raman Amplification," *Journal of Lightwave Technology*, vol. PP, no. 99, 2015.
- [31] I. Tavakkolnia and M. Safari, "Signalling over nonlinear fibre-optic channels by utilizing both solitonic and radiative spectra," in *Networks and Communications (EuCNC), 2015 European Conference on*, 2015, pp. 103-107.
- [32] S. T. Le, S. Wahls, D. Lavery, J. E. Prilepsky, and S. K. Turitsyn, "Reduced Complexity Nonlinear Inverse Synthesis for Nonlinearity Compensation in Optical Fiber Links," in *2015 European Conference on Lasers and Electro-Optics - European Quantum Electronics Conference*, Munich, 2015, p. CI_3_2.
- [33] S. Wahls, S. T. Le, J. E. Prilepsky, H. V. Poor, and S. K. Turitsyn, "Digital Backpropagation in the Nonlinear Fourier Domain," presented at the Proc. IEEE SPAWC, Stockholm, Sweden, 2015.
- [34] A. D. Ellis, S. T. Le, M. E. McCarthy, and S. K. Turitsyn, "The Impact of Parametric Noise Amplification on Long Haul Transmission Throughput," presented at the ICTON, Budapest, Hungary, paper We.D1.5, 2015.